

## THE PRESSURE-FLOW CHARACTERISTIC OF CIRCULAR MOLDING CHANNELS WITH A NONISOTHERMAL FLOW OF THERMOPLASTIC POLYMERS

L. M. Ul'ev

UDC 532.135:678.027

*The article contains results of a numerical investigation of the pressure-flow characteristic of high-viscosity flows for different rates of heat transfer with the environment. The effect of nonmonotonicity of the characteristic  $\Delta P(V_0)$  on the stability of operation of the die head of extrusion apparatus is discussed.*

In extrusion production and processing of thermoplastic materials, polymer melts are pressed through dies, fine molding channels, which are of a cylindrical shape in the production of strands, rods, and granules. Since polymer solutions are high-viscosity liquids, because of substantial energy dissipation and a strong dependence of viscosity on temperature, in the dies the liquid flows under high gradients of temperature and viscosity. In the die at different flow rates of the melt and different conditions of heat transfer with the environment, the viscosity distribution will determine the pressure-flow characteristic of the die. With this characteristic known, it is possible to choose optimal process and design parameters of extrusion [1].

The pressure-flow characteristics of dies were studied in [2] for a De Haven fluid at various melt temperatures, but the authors only considered an isothermal flow. In nonisothermal viscous flows the pressure-flow characteristics were considered earlier mainly for special cases of a flow in a stabilized heat-transfer region [3, 4] or for a flow with negligible dissipation [5-7]. In these studies limiting boundary conditions or those with a preset wall temperature [3, 4-7] or the second-kind boundary conditions [5] were chosen. In [8-11] the characteristics were obtained for the third-kind boundary conditions within the initial thermal length, but the temperature across the channel was assumed constant, which allowed the authors to include longitudinal convective heat transfer only as an average, while transverse convective heat transfer was completely ignored, just as in all the works mentioned earlier. In [5-11] nonmonotonic pressure-flow characteristics were obtained, and in [11] they were found only for a plane channel. In [12] the isothermal characteristic  $\Delta P(V_0)$  was studied for a flow of oil in a circular capillary with thermal boundary conditions of the first kind and flow with an adiabatic wall. In that work both energy dissipation and transverse convective heat transfer were taken into consideration. The obtained characteristic  $\Delta P(V_0)$  is strictly monotonic, but the Gnome-Griffith numbers are 3-4 orders of magnitude smaller as compared with the polymer flow at the same velocities.

In the present work the pressure-flow characteristic is studied for a flow of thermoplastic polyurethane (TPU) melts in circular cylindrical channels at various rates of heat transfer with the environment.

Within the range of processing parameters, melts of glue-type TPU (Vitur T-12K, etc.) behave as Newtonian fluids with the viscosity-temperature relation [13]

$$\mu(T) = \mu_0 \exp \left[ \frac{E}{R} \left( \frac{1}{T} - \frac{1}{T_0} \right) \right], \quad (1)$$

where  $\mu_0 \approx 10^3$  Pa·sec,  $E \approx (10^5 - 3 \cdot 10^5)$  J/mole,  $T_0 = 463^\circ$ .

For practical flow rates  $Q = 10^{-5}$  to  $10^{-7} \text{ m}^3/\text{sec}$  and physical properties of the melt  $\rho \approx 1200 \text{ kg/m}^3$ ,  $\alpha \approx 10^{-7} \text{ m}^2/\text{sec}$ , and  $r_0 \approx (1 - 3) \cdot 10^{-3} \text{ m}$ , we have  $\text{Re} \ll 10^{-2}$ ; then the mechanical relaxation length is equal to [14]

$$l_1 \approx V_0 r_0^2 \rho / \mu \approx 10^{-6} \text{ m}, \quad (2)$$

and the thermal relaxation length is equal to [14]

$$l_2 \approx V_0 r_0^2 \rho c / \lambda \approx 10 \text{ m}, \quad (3)$$

i.e., at the channel inlet the velocity profile can be assumed to be developed and to correspond to the temperature distribution.

If the fluid is led to the channel with a homogeneous temperature distribution, the main changes in the velocity distribution occur in the section where a low-viscosity shear layer is formed [14]:

$$l_3 \sim \text{Pe} \cdot \text{Gn}^{-3/2} r_0 \approx 10^{-1} \text{ m}. \quad (4)$$

The quantity  $L_0 = l_3$  is the characteristic longitudinal dimension for a flow with a homogeneous initial temperature distribution, and  $L_0 = l_2$  is the characteristic dimension for a flow with a previously developed low-viscosity thermal layer, for example, in the flow in the conic part of the die [15], and the radius of the channel is the characteristic transverse dimension.

Using these quantities, it is possible to evaluate the derivatives in the equations of convective heat transfer [1]  $\partial/\partial r \sim 1/r_0$ ;  $\partial/\partial z \sim 1/L_0$ .

Under axisymmetric boundary conditions, the geometry of the channel allows the flow to be considered axisymmetric, and Eqs. (2) and (3) show that the velocity distribution will always have time to adjust to the temperature distribution. In this case the discontinuity equation estimates the radial component of the velocity  $V_r \approx V_z(r_0/L_0) = o(V_z)$ , i.e., in the equations of motion the terms with  $V_r$  can be neglected, but, as is shown in [15, 16], in the equation of heat transfer, convective heat transfer cannot be neglected.

The above assumptions, evaluation of the derivatives, the number  $\text{Pe} \approx 10^5$ , and the smallness of  $\text{Re}$  allow us to simplify the steady-state system of equations of hydrodynamics and heat transfer [1], which, in terms of the dimensionless variables and parameters

$$\xi = \frac{r}{r_0}, \quad \chi = \frac{z}{r_0}, \quad \Pi = \frac{(P - P_0) r_0}{\mu_0 V_0}, \quad V_0 = \frac{Q}{\pi r_0^2}, \quad \beta = \frac{RT_0}{E}, \quad \Theta = \frac{T - T_0}{\Delta T}, \quad v = \frac{V_z}{V_0},$$

$$\omega = \frac{V_r}{V_0}, \quad m = \exp\left(-\frac{\Theta}{1 + \beta\Theta}\right), \quad \text{Gn} = \frac{\mu(T_0) V_0^2}{\lambda \Delta T}, \quad \text{Bi} = \frac{Kr_0}{\lambda}, \quad \text{Pe} = \frac{V_0 r_0}{\alpha}, \quad \text{Re} = \frac{\rho V_0 r_0}{\mu_0},$$

$$\Delta T = \left. \mu(T) \right|_{T=T_0} / \left. \left( \frac{\partial \mu}{\partial T} \right) \right|_{T=T_0} = \beta T_0,$$

will be written as

$$\frac{\partial \Pi}{\partial \chi} = \frac{1}{\xi} \frac{\partial}{\partial \xi} \left( \xi m \frac{\partial v}{\partial \xi} \right), \quad (5)$$

$$\frac{1}{\xi} \frac{\partial}{\partial \xi} (\xi \omega) + \frac{\partial v}{\partial \chi} = 0, \quad (6)$$

$$\frac{1}{\xi} \frac{\partial}{\partial \xi} (\xi \omega \Theta) + \frac{\partial}{\partial \chi} (\nu \Theta) = \frac{1}{\text{Pe}} \frac{1}{\xi} \frac{\partial}{\partial \xi} \left( \xi \frac{\partial \Theta}{\partial \xi} \right) + \frac{\text{Gn}}{\text{Pe}} m \left( \frac{\partial \nu}{\partial \xi} \right)^2, \quad (7)$$

$$0 \leq \xi < 1, \quad 0 \leq \chi \leq L/r_0,$$

The boundary conditions

$$\frac{\partial \Theta}{\partial \xi} = 0, \quad \frac{\partial \nu}{\partial \xi} = 0, \quad \xi = 0, \quad 0 \leq \chi \leq L/r_0, \quad (8)$$

$$\nu = 0, \quad \omega = 0, \quad \frac{\partial \Theta}{\partial \xi} = -\text{Bi} (\Theta - \Theta_a), \quad \xi = 1, \quad 0 \leq \chi \leq L/r_0, \quad (9)$$

$$\Theta = 0, \quad \Pi = 0, \quad 0 < \xi < 1, \quad \chi = 0, \quad (10)$$

and the conditions of the flow constancy are written as

$$2 \int_0^1 \nu \xi d\xi = 1. \quad (11)$$

For solution of the formulated problem use will be made of the method developed in [15, 16], in which the flow region is divided into  $N$  concentric cylindrical layers and in the cross-section of each  $i$ -th layer the viscosity is assumed constant and equal to  $m_i$  taken at the layer cross section-average temperature. In this approach, system of Eqs. (6)-(8) is divided into  $3N$  equations, and  $5(N - 1)$  conditions of conjugation of velocities, temperatures, and shear stresses at the boundaries of the layers are added to boundary conditions (9)-(12). After integration of Eqs. (6) and (7) with respect to  $\xi$  and averaging (9) over the cross-sectional area of the layer, we obtain a system of ordinary differential equations describing the average temperatures in the layers and the pressure:

$$\frac{d\bar{\Theta}_i}{d\chi} = \frac{2}{\bar{\nu}_i d_i} [\xi_i (\omega_i - \text{St}_i) (\bar{\Theta}_i - \bar{\Theta}_{i+1}) - (\bar{\Theta}_i - \bar{\Theta}_{i-1})] + \frac{\text{Gn } m_i}{\text{Pe } \bar{\nu}_i} \overline{\left( \frac{\partial \nu}{\partial \xi} \right)^2}, \quad (12)$$

$$\frac{d\Pi}{d\chi} = -8 \left( \sum_{i=1}^N \frac{\xi_i^4 - \xi_{i-1}^4}{m_i} \right)^{-1} = -8/S, \quad (13)$$

where

$$\bar{\nu}_i = \frac{1}{S} \left( \frac{d_i}{m} + 2 \sum_{K=1}^{N-i} \frac{d_{i+K}}{m_{i+K}} \right), \quad \text{St}_1 = \frac{1}{\xi_1} \left( \frac{\xi_2^2}{d_2} \ln \frac{\xi_2}{\xi_1} - \frac{1}{2} \right)^{-1}, \quad d_i = \xi_i^2 - \xi_{i-1}^2,$$

$$\text{St}_i = \frac{1}{\xi_i} \left( \frac{\xi_{i+1}^2}{d_{i+1}} \ln \frac{\xi_{i+1}}{\xi_i} - \frac{\xi_{i-1}^2}{d_i} \ln \frac{\xi_i}{\xi_{i-1}} \right)^{-1}, \quad \text{St}_N = \left( \frac{1}{2} - \frac{\xi_{N-1}^2}{d_N} \ln \frac{\xi_N}{\xi_{N-1}} + \frac{1}{\text{Bi}} \right)^{-1},$$

$$\omega_i = -\frac{1}{2\xi_i} \sum_{K=1}^i d_K \frac{d\bar{\nu}_K}{d\chi}.$$

Here  $i = 1, 2, \dots, N$  and then  $\bar{\Theta}_{N+1} = \Theta_a$ . The derivative  $d\nu_i/d\chi$  is found from the distribution  $\nu_i(\xi)$ :

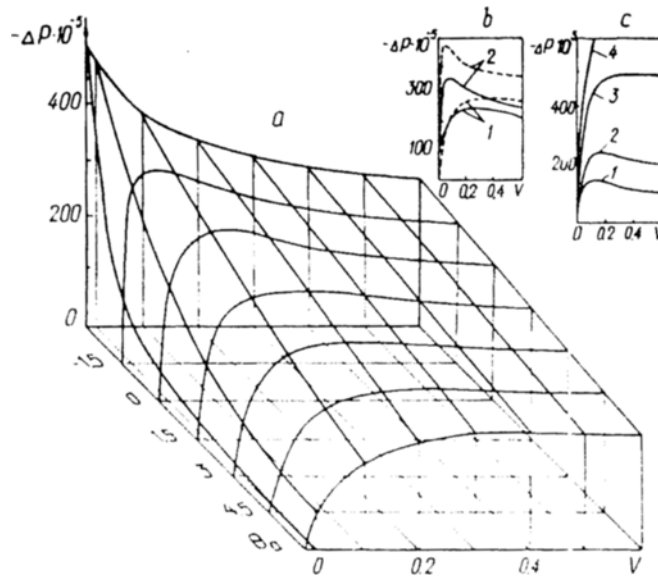


Fig. 1. Pressure drop in cylindrical channel: a) versus flow velocity and the ambient temperature at  $Bi = 3.75$ ; b) solid curves for flow with  $Bi = 3.75$ ; dashed curves with  $Bi = 15$ : 1) for  $\Theta_a = 3.2$ ; 2)  $\Theta_a = 1.5$ ; c) flow with adiabatic wall: 1)  $\beta = 0.77 \cdot 10^{-3}$ , 2)  $1.44 \cdot 10^{-2}$ , 3)  $3.88 \cdot 10^{-2}$ , 4)  $4.7 \cdot 10^{-2}$ .  $P$ , Pa;  $V$ , m/sec.

$$v_i(\xi) = \frac{2}{S} \left( \frac{\xi_i^2 - \xi^2}{m_i} + \sum_{K=1}^{N-i} \frac{d_{i+K}}{m_{i+K}} \right), \quad (14)$$

and the expressions  $dm_i/dx = -(m_i/(1 + \beta\bar{\Theta}_i))(d\bar{\Theta}_i/dx)$ ,  $\overline{(\partial v/\partial \xi)^2}$  are also determined from (14).

In [16] it is shown that by changing the heat transfer rate at the boundary, it is possible to control the distributions of temperature, velocity, and pressure in a channel with high-viscosity flows. We will study how the characteristic  $\Delta P(V_0)$  behaves in a channel section with dimensions  $L = 0.12$  m and  $r_0 = 1.5 \cdot 10^{-3}$  m for  $a = 8 \cdot 10^{-8}$  m<sup>2</sup>/sec,  $\beta = 1.44 \cdot 10^{-2}$ , and  $Bi = 3.75$ . For do this, we will consider some steady-state flows with different average velocities. At the boundary the heat transfer rate will be changed by setting different values of  $\Theta_a$ .

In the range of  $\Theta_a$  studied, irrespective of the initial direction of the heat flux, i.e., for both  $\Theta_a > 0$  and  $\Theta_a < 0$ , the pressure-flow characteristic has an extremum (Fig. 1a), i.e., after a certain value of the flow rate is exceeded, the hydraulic resistance of the channel decreases.

This result becomes clear if we consider the dependence of the pressure drop  $\Delta P = P - P_0$  on the longitudinal coordinate. First, the effect of heat transfer at the boundary is excluded, and the curve  $\Delta P(V_0)$  is considered for flow with an adiabatic wall (Fig. 1c).

At low flow rates, the rates of shear are small, dissipation is insignificant, and all heat released can be distributed uniformly over the cross-section of the flow. Although, in general, the temperature of the fluid rises insignificantly along the channel, the velocity profile differs only slightly from the Poiseuille distribution (see Fig. 3), which leads to only a slight deviation of the characteristic  $\Delta P(z/r_0)$  from a linear function (Fig. 2a). As the flow rate increases, this behavior is observed until a low-viscosity boundary layer is formed within the channel. The formation of this layer can be explained by the fact that with an increase in the flow rate, in the peripheral flow the velocity gradient increases and so does the energy dissipation, which, because of the low thermal conductivity of polymers, cannot relax during the residence time of the melt in the channel. As the temperature rises at the wall, the viscosity decreases there, and the velocity profile becomes more filled, i.e., the rate of shear in the periphery increases, which results in localization of the heat release. Meanwhile, the modulus of the pressure gradient decreases, and the curve  $\Delta P(\chi)$  markedly deviates from the line after the low-viscosity layer appears (Fig. 2a). The velocity at which the low-viscosity layer appears in the channel can be estimated from Eq. (4), assuming

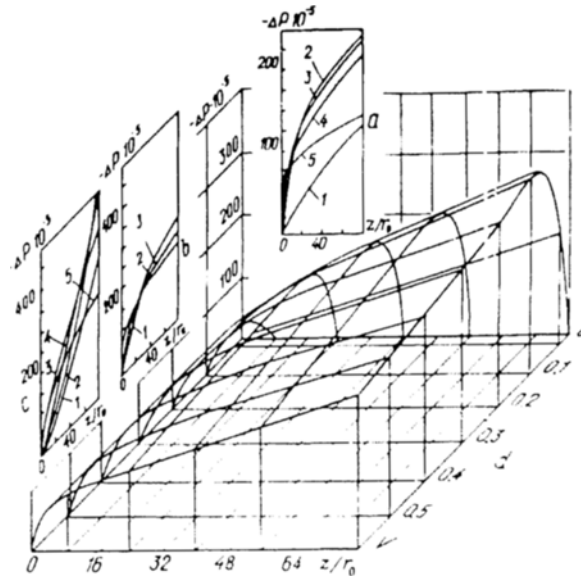


Fig. 2. Pressure distribution along the channel: a) flow with adiabatic wall (1)  $V_0 = 1.44 \cdot 10^{-2}$  m/sec, 2)  $1.44 \cdot 10^{-1}$ , 3)  $2.82 \cdot 10^{-1}$ , 4) 0.52, 5) 3 m/sec; b) flow at  $\Theta_a = 3$  (1)  $V_0 = 8.48 \cdot 10^{-2}$  m/sec, 2)  $V_0 \sim (1.4 - 4) \cdot 10^{-1}$  m/sec, 3) 1.13 m/sec; c) flow at  $\Theta_a = -3$  (1)  $V_0 = 1.13 \cdot 10^{-3}$  m/sec, 2)  $4.24 \cdot 10^{-3}$  m/sec, 3)  $1.41 \cdot 10^{-2}$  m/sec, 4)  $8.41 \cdot 10^{-2}$  m/sec, 5) 0.71 m/sec; d) pressure versus longitudinal coordinate and mean flow velocity for  $\Theta_a = 0$ .

$l_3 = L$ . In this case  $V_0 \sim 3-4$  cm/sec, which agrees well with numerical results. It is clear that starting from this velocity, substantial nonlinearity appears in the pressure-flow characteristic as well (Fig. 1c).

It is in this region of formation of the low-viscosity boundary layer that the main restructuring of the velocity profile occurs; therefore, the inclusion of transverse convective heat transfer becomes very important. As was shown earlier [16], even for low velocities the ratio  $q_{vr}/q_{\lambda r}$  can be  $\sim 10$ , and, as is shown by calculations, for high  $V_0$  this ratio can reach several tens, so the neglect of transverse convective heat transfer will result in an incorrectly determined temperature distribution and consequently, in an incorrectly calculated pressure drop.

For higher flow rates, in the initial flow section the modulus of the pressure gradient is high, as is the dissipation, which results in the rapid formation of a high-temperature low-viscosity layer and in a nearly rectangular velocity profile (Fig. 3), which in the subsequent flow enhances the effects described. Indeed, when the profile of the longitudinal component of the velocity is flattened, the radial components are positive, which prevents convective heating of the flow core. There dissipation is almost absent, since in the central region  $dv/dr \approx 0$  (Fig. 3) and with the short residence time of the melt in the channel this region is heated insignificantly by heat conduction. As a result, the central high-viscosity flow core is surrounded by a low-viscosity liquid layer, and in the channel a high-temperature rod-like flow is developed with a low pressure gradient. Eventually, the pressure drop in the channel can be lower than in flow with low flow velocity, though at the channel inlet the pressure drop is higher in the former case (Fig. 2a). As a result, in a nonisothermal flow the pressure-flow characteristic is nonmonotonic.

In the case of heat transfer with the environment, the nonisothermality of the flow is determined not only by dissipation but also by heat transfer at the boundary. At  $\Theta_a = 0$  for flow at low velocities, the temperature is distributed almost uniformly across the channel (Fig. 3), but it is lower than the temperature at  $Bi = 0$ , since some of the energy is transferred to the environment. There the pressure falls more rapidly and over the length of the channel  $\Delta P$  is higher than it was earlier. At high flow velocities a high-temperature boundary layer is also formed, but it is slightly wider than the boundary layer at  $Bi = 0$  (Fig. 3), since, as a result of heat transfer near the wall, the temperature falls, and the viscosity increases, which leads to a more-extended velocity profile, and there the dissipation is substantial over the largest part of the channel. Starting from a certain  $V_0$ ,  $\Delta P$  decreases, but for any

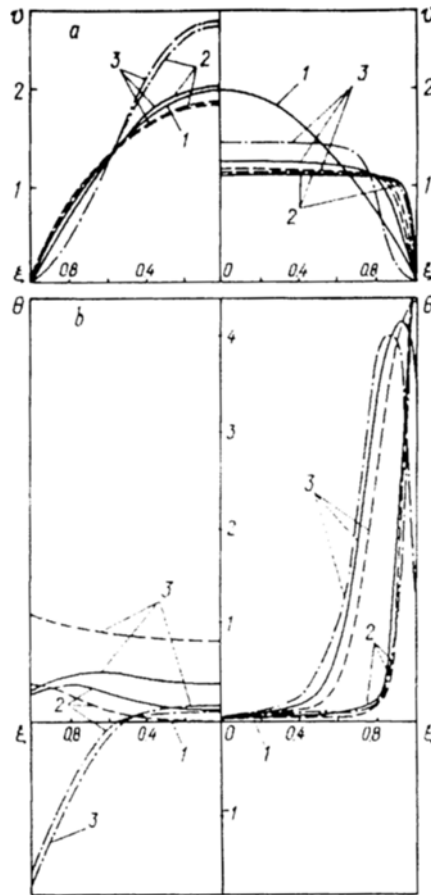


Fig. 3. Distributions of (a) dimensionless longitudinal velocity and b) dimensionless temperature across the channel. The left-hand half, for low velocities  $V_0 \sim 0.1 - 0.3$  m/sec. Solid curves  $\Theta_a = 0$ , dot-dash curves  $\Theta_a = -3$ , dashed curves  $Bi = 0$ : 1) for  $\chi = 0$ , 2) 7.8, 3) 80.

$V_0$  the condition  $|\Delta P(\Theta_a = 0)| > |\Delta P(Bi = 0)|$  is satisfied (see Fig. 2). It is interesting to note that for short channels ( $L < 15r_0$ ) the pressure-flow function increases monotonically (Fig. 2d). For high  $V_0$ , it is there that the low-viscosity layer is developed, and, as the flow rate increases,  $|\nabla P|$  also increases.

For low flow velocities and  $\Theta_a > 0$  the liquid is heated uniformly; therefore, the pressure drop is slower than it was earlier (Fig. 2b); for high velocities less energy is spent on formation of the thermal boundary layer, because of which  $|\Delta P(\Theta_a > 0)| > |\Delta P(\Theta_a = 0)| \forall V_0$  (see Fig. 1a).

In the case of  $\Theta_a < 0$ , the melt is cooled at the periphery at low flow velocities, the velocity profile is extended, and energy dissipation becomes important in the central region as well. Therefore, the liquid is cooled nonuniformly over the cross section (Fig. 3); the central part is even overheated, but due to an increase in  $\mu$  at the periphery,  $|\Delta P|$  grows along the channel (see Fig. 2c) (the curve of  $\Delta P(\chi)$  is convex downward). For high  $V_0$ , the temperature is substantially lower at the wall than it is for other  $\Theta_a$  (see Fig. 3); therefore, the condition  $|\Delta P(\Theta_a > 0)| < |\Delta P(\Theta_a = 0)| \forall V_0$  is satisfied (see Fig. 1a). It should be noted that at  $\Theta_a < 0$ , as  $V_0$  increases, very soon the rate of dissipation starts to prevail over the heat release to the environment, therefore the maximum value of  $|\Delta P(V_0)|$  is shifted leftward.

It should be noted that at low flow velocities the relation  $|\Delta P(\Theta_a)|$  mainly follows the function  $\mu = \mu(T)$ , since dissipative effects are unimportant there, and for a high-temperature flow  $|\Delta P(\Theta_a)|$  is almost nonlinear (see Fig. 1).

At constant  $\Theta_a$  the rate of heat transfer with the environment is determined by the value of  $Bi$ . For  $\Theta_a > 0$ , an increase in  $Bi$  results in the fact that at low  $V_0$  the liquid is heated more intensely and  $|\Delta P|$  decreases.

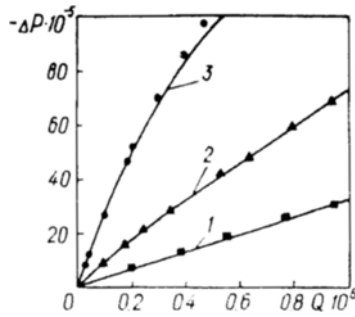


Fig. 4. Comparison of numerical results with experimental data [12] for Newtonian flow of oil in channel with  $L = 4.54 \cdot 10^{-2}$  and  $r_0 = 1.3 \cdot 10^{-4}$  m. Solid curves, calculation; dots, experimental data: 1)  $T_0 = 363.55$  K, 2) 336.05, 3) 310.75.  $Q$ ,  $m^3/sec$ .

For high velocities, due to dissipation the temperature at the wall becomes higher than  $\Theta_w$  and the heat flux  $q = Bi(\bar{\Theta}_N - \Theta_w)$  changes its sign and becomes larger in absolute value than it is at lower Bi, which results in an increase in  $|\Theta P(V_0)|$  (see Fig. 1b). It is clear that at  $\Theta_w < 0$  an increase in Bi will only lead to an increase in  $|\Delta P|$  for any  $V_0$  (see Fig. 1b).

The value of  $\beta$  has a great effect on the shape of the curve  $|\Delta P(V_0)|$ . At  $\beta \rightarrow \infty$ ,  $Gn \rightarrow 0$ , i.e., the intensity of heat release does not affect the flow dynamics and  $|\Delta P(V_0)|$  tends to the Poiseuille relation. As  $\beta$  decreases,  $Gn$  and  $\mu(T)$  increase, the value of the maximum attainable  $|\Delta P|$  decreases, and this pressure is attained at lower velocities (see Fig. 1c).

The effects considered that can occur in processing of polymers can give rise to unexpected phenomena. For example, if in submerged granulation an unheated die board is used, as a rule, a situation arises in which several tens of holes are clogged by solidified melt and through the other 1–3 holes the melt is fed at the same flow rate within substantial changes in the pressure in the apparatus.

This situation can arise as a result of some, possibly random, decrease in the flow velocity in some of the dies, which will result in a longer residence time of the melt in the die. Due to heat transfer, the melt is cooled more rapidly as compared with the other dies, which results in a decrease in its velocity etc., until the flow in these holes stops. Meanwhile, in the other dies the velocity increases accordingly, the energy dissipation increases,  $|\nabla P|$  decreases, etc. Eventually, the entire melt will flow through a few holes, which will result in disruption of the process; therefore, the possibility of this phenomenon should be taken into consideration in designing apparatus for processing of thermoplastics.

This phenomenon can be avoided by heating the die channels. At  $\Theta_w > 0$ , negative feedback between the flow characteristics and heat transfer appears, i.e., if the velocity in the channel decreases for some reason, it will not lead to an increase in the viscosity, and, because of longer residence time of the melt in the channel, the melt will be heated at the periphery, which will result in restoration of the previous operating conditions. Each die should be heated separately, and the process parameters for steady operation can be chosen from the curves shown in Fig. 1.

The adequacy of the suggested model of the flows of melts has been verified by comparison of earlier published data with the results that we obtained for the conditions indicated in the publications. In Fig. 4, one can see data for a liquid flow with a temperature-dependent viscosity [12]  $\mu = 10^6 \rho [\exp(A/T^b) - 0.6]$ , where  $A = 1.372 \cdot 10^{10}$  and  $b = 3.81$ . The comparison shows good agreement.

## NOTATION

$a$ , thermal diffusivity,  $m^2/sec$ ;  $c$ , specific heat,  $J/(kg \cdot K)$ ;  $E$ , activation energy of viscous flow,  $J/mole$ ;  $K$ , heat transfer coefficient,  $W/(m^2 \cdot K)$ ;  $P$ ,  $P_0$ , instantaneous pressure and pressure at the channel inlet, Pa;  $R$ , universal gas constant,  $J/(mole \cdot K)$ ;  $Q$ , flow rate,  $m^3/sec$ ;  $q_{vr}$ ,  $q_{\lambda r}$ , transverse convective and transverse conductive

heat fluxes,  $W/m^2$ ;  $r$ ,  $r_0$ , radial coordinate and radius of the channel, m;  $T$ ,  $T_0$ , current temperature of the melt and temperature of the melt at the channel inlet, K;  $V_0$ , velocity, m/sec;  $z$ , longitudinal coordinate, m;  $\lambda$ , thermal conductivity,  $W/(m \cdot K)$ ;  $\mu$ , dynamic viscosity, Pa·sec;  $\rho$ , density,  $kg/m^3$ ;  $Bi$ , Biot number;  $Gn$ , Gneme–Griffith number;  $Pe$ , Peclet number;  $Re$ , Reynolds number;  $St_i$ , Student number for the  $i$ -th layer. Subscripts:  $a$  refers to the environment;  $i$ , the layer number;  $r$ ,  $z$ , the radial and longitudinal components of the vector.

## REFERENCES

1. Z. Tadmor and K. Gogos, Theoretical Fundamentals of Polymer Processing [Russian translation], Moscow (1984).
2. V. I. Pervadchuk, I. O. Glot, V. I. Yankov, and L. B. Mal'kov, *Khim. Volokna*, No. 3, 36-37 (1985).
3. S. A. Bostandzhiyan, A. G. Merzhanov, and S. I. Khudyaev, *Dokl. Akad. Nauk SSSR*, No. 1, 133 (1965).
4. S. L. Benderskaya, B. M. Khusid, and Z. P. Shul'man, *Izv. Akad. Nauk SSSR, Mekh. Zhidk. Gaza*, No. 3, 3-10 (1980).
5. V. I. Naidenov, A. M. Brener, V. V. Dil'man, and A. A. Maksimov, in: Current Heat and Mass Transfer Problems in Chemical Engineering [in Russian], Materials of the International Workshop, Pt. 3, Minsk (1987), pp. 116-123.
6. V. I. Naidenov, *Teplofiz. Vysok. Temp.*, **24**, No. 1, 82-88 (1986).
7. V. I. Naidenov, A. M. Brener, and V. V. Dil'man, *Teor. Osnovy Khim. Tekhnol.*, **23**, No. 3, 300-308 (1989).
8. A. G. Merzhanov and A. M. Stolin, *Prikl. Mat. Tekhn. Fiz.*, No. 1, 65074 (1974).
9. A. Ya. Malkin and A. E. Chalykh, *Diffusion and Viscosity of Polymers. Measuring Methods* [in Russian], Moscow (1979).
10. N. B. Aleksapol'skii and V. I. Naidenov, *Teplofiz. Vysok. Temp.*, **17**, No. 4, 783-791 (1979).
11. Y. T. Shan and J. R. A. Pearson, *Chem. Eng. Sci.*, **29**, No. 6, 1485-1493 (1974).
12. J. L. Duba, E. E. Klaus, and S. C. Lin, *Ind. Eng. Chem. Res.*, **27**, No. 2, 352-361 (1988).
13. V. G. Ponomarenko, G. F. Potebnya, L. M. Ul'ev, et al., *Inzh.-Fiz. Zh.*, **59**, No. 1 (1990), Deposited at VINITI, Reg. No. 1224-B90, March 5, 1990.
14. H. Ockendon, *J. Fluid Mech.*, **93**, Pt. 4, 737-746 (1979).
15. L. M. Ul'ev, *Teor. Osnovy Khim. Tekhnol.*, **26**, No. 2, 243-253 (1992).
16. V. G. Ponomarenko, G. F. Potebnya, and L. M. Ul'ev, *Prom. Teplotekhn.*, **7**, No. 1, 9-16 (1985).